Title: Whole brain mapping of transcranial electrical stimulation-induced effects by BOLD-fMRI in rats

Authors: Mihaly Voroslakos*, Tanzil Mahmud Arefin*, Jiangyang Zhang, Leeor Alon and Gyorgy Buzsaki
* These authors contributed equally.

Synopsis: Transcranial Electrical Stimulation (TES) is a noninvasive method that can modulate neuronal activity. Despite 20 years of intensive research, the basic mechanisms, and the extent of TES influence on brain functions is still not well understood. To gain a better understanding of the TES effects, we combined neurostimulation with BOLD-fMRI in rats. We have designed an MR-compatible TES setup, including a deuterium-based stimulation electrode system. Our results revealed BOLD responses to TES and altered cortical and cortico-subcortical network responses induced by a variety of stimulation patterns and intensities.

Summary of main findings: TES can affect cortical and cortico-subcortical functional networks in anesthetized rats. TES can induce stimulation intensity-dependent changes in prefrontal, default mode, cortico-hippocampal and thalamo-cortical networks.

Introduction: Non-invasive brain stimulation techniques provide an unprecedented opportunity to probe and modify brain circuits in health and disease. These methods have contributed numerous insights into brain function and are now widely used in clinical settings, including rehabilitation and treatment of mental disorders[1]. Transcranial Electrical Stimulation (TES) has gained popularity because of its convenience (the required equipment is portable) and potential as a chronic therapy[2]. The efficacy of TES depends on stimulation intensity, duration, polarity, and electrode montage[3]. TES-induced electric fields are believed to be stronger closest to the stimulation electrode[4]. However, modeling studies suggest that unpredicted areas such as the brainstem can also be stimulated, due to the current shunting effects of the cerebrospinal fluid[4]. In vitro studies have shown a linear relationship between applied field and physiological response[5]. However, this dose-response relationship is more complex in vivo[6] (Fig. 1), and perhaps even more so in humans due to cortical folding and different scalp and skull thickness[4].
Integration of TES with magnetic resonance imaging (MRI) techniques provides a tool to directly perturb neuronal functions while monitoring brain activities[7,8]. It enables researchers to study how TES modulates targeted brain regions, and how modulation occurs through anatomical and functional connectivity[9]. Varying stimulation pattern and intensity can provide critical insight for dose-response. The goal of our study is to quantify TES-affected brain regions using blood oxygenation level dependent (BOLD) resting state functional MRI (fMRI) in anesthetized rats and compare the effective intensities of stimulation on functional connectivity of different brain areas.

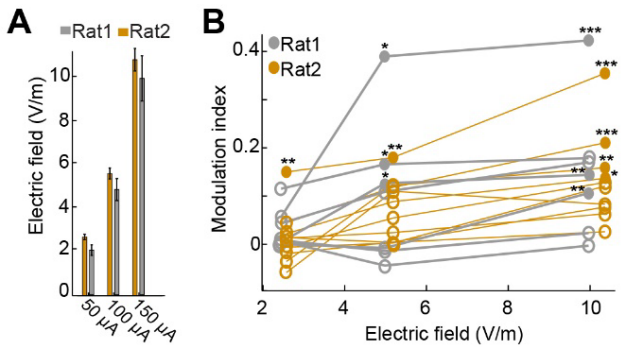

Figure 1. Dose-response relationship in rats. A) Electric field measured in the hippocampus. Increasing stimulation intensities induced higher electric fields. To measure electric fields, sinusoidal stimulation was applied (peak-to-peak intensity: 50, 100 and 150 µA at 100 Hz). **B)** Firing rate changes as a function of TES intensity (n=2 rats, n=200 trials for each intensity, 2s on – 2s off). Each line corresponds to a well isolated single neuron. Note increasing fraction of significantly modulated neurons at higher electric fields (Wilcoxon rank sum test).

Methods: fMRI data were acquired with T_2^*-weighted single-shot GE-EPI sequence on urethane anesthetized rats (N=3, 1.4 g/kg, IP). Rat brain excluding the cerebellum was covered using 23 axial slices with the following parameters: TE/TR=13.4/(1500 or 2200)ms (TES or rsfMRI), 300 repetitions and resolution = 0.23 x 0.23 x 0.8mm. 500-ms constant current pulses were applied at every 33, 6.6, 4.4 or 2.2 seconds (100, 33, 50 and 100 %, respectively). Resting-state (rs)-fMRI data were acquired between TES pulses. Physiological parameters (rectal temperature, respiratory rate, and oxygen saturation) were monitored.

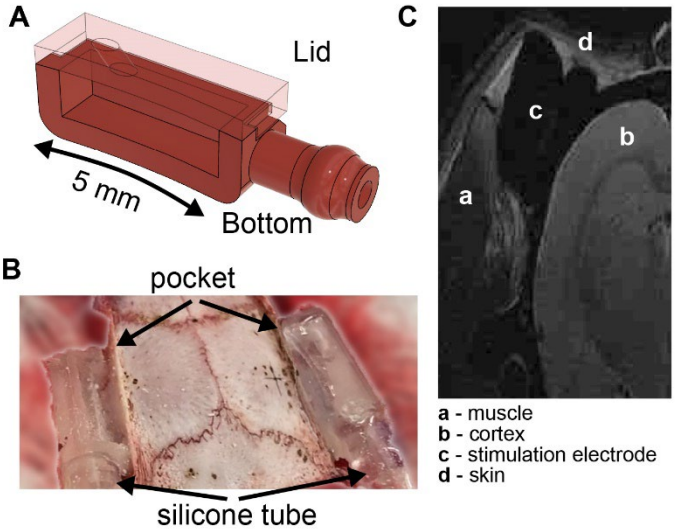

Figure 2. MR artifact-free transcranial stimulation system. A) Stimulation pocket consists of a bottom part and a lid. **B)** Intraoperative photograph of stimulation system. Left pocket: bottom part is attached to the skull. Right pocket: lid is attached to the bottom part and covered with dental cement. Note the silicone tube attachment. **C)** T2 weighted image of the rat's head. Note the location of the deuterium stimulation electrode (c) above visual and auditory cortices (b).

Electrical stimulation was delivered using our custom designed, 3D-printed pockets (2x5 mm, Fig. 2A). The pocket consists of a bottom part and a lid. The bottom part was secured to the temporal bone bilaterally with dental cement, and the lid with a hole was attached to the bone/bottom to create a watertight seal (Fig. 2B). The pockets were filled with deuterium using a 2ml syringe. To increase conductivity, NaCl was added to the deuterium (5%). To reduce MR artifacts (e.g. RF heating and eddy currents on the wires, Fig. 2C), twisted copper wires were inserted inside the silicone tube 20cm away from the brain (Fig. 3). Resistance of stimulation electrode was monitored regularly throughout the experiments. Electrical stimulation was delivered prior to the start of image acquisition (before the RF pulses) to reduce the interference between TES currents and MR signal (Fig. 3).

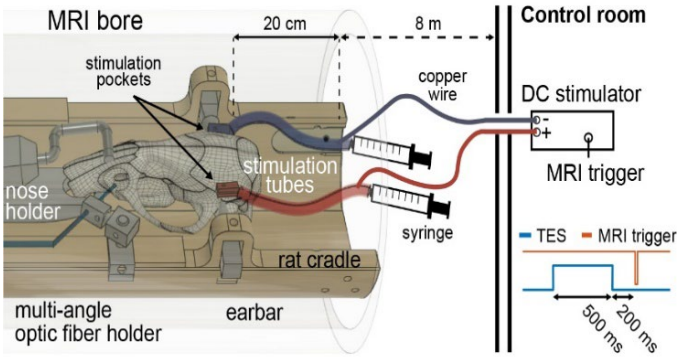

Figure 3. Concurrent TES-fMRI in anesthetized rats. Schematic of our custom designed 3D-printed head-fixation setup. Animal is inside the bore (only skull is shown). Optic fiber is placed in front of its eye. 3D-printed stimulation pockets are attached to the temporal bones bilaterally. The pockets are filled with deuterium using silicon tubes attached to syringes (blue and red tubes). Twisted copper wires are inserted into the silicon tubes 20 cm away from the pockets. Isolated stimulator delivers 500-ms TES and triggers image acquisition 200 ms after the offset of TES.

Different duty cycles were used to determine the TES-induced time courses of the BOLD signal. In addition, 3 different intensities were applied to establish a dose response (Fig. 4A,B).

The fMRI data analysis included the following steps: EPI and structural image of each subject were normalized to a template space – Swanson's rat atlas (down-sampled to 36 structures)[10]. Using these 36 nodes, whole brain functional connectivity (FC) matrix was mapped (average of 3 rats) to identify the networks that are affected by TES. Pearson's correlation coefficient for each connection was calculated in subject's space and normalized to a z-score using Fisher's r-to-z transformation.

After the MRI data acquisition, electrophysiology recording was performed from the hippocampus using a silicon probe. Neuronal activity was recorded for 30 min (baseline) followed by 300 trials of electrical stimulation (500-ms TES pulses followed by 2 s stimulation free epochs, two polarities at 500 µA intensity).

Results: Several brain regions, including somatosensory/motor cortices, hippocampus, and thalamus showed BOLD responses to TES. Overall, we observed stimulation intensity-dependent changes in rat brain FC networks (Fig. 4C). Within the cortex, FC strength was strongly modified particularly in the prefrontal and default mode network (blue and red boxes) in response to the stimulation intensities from 100 µA to 250 and 500 µA. However, the cortico-hippocampal (black box) and thalamo-cortical (purple box) networks exhibited stronger modifications at intensities higher than 100 µA.

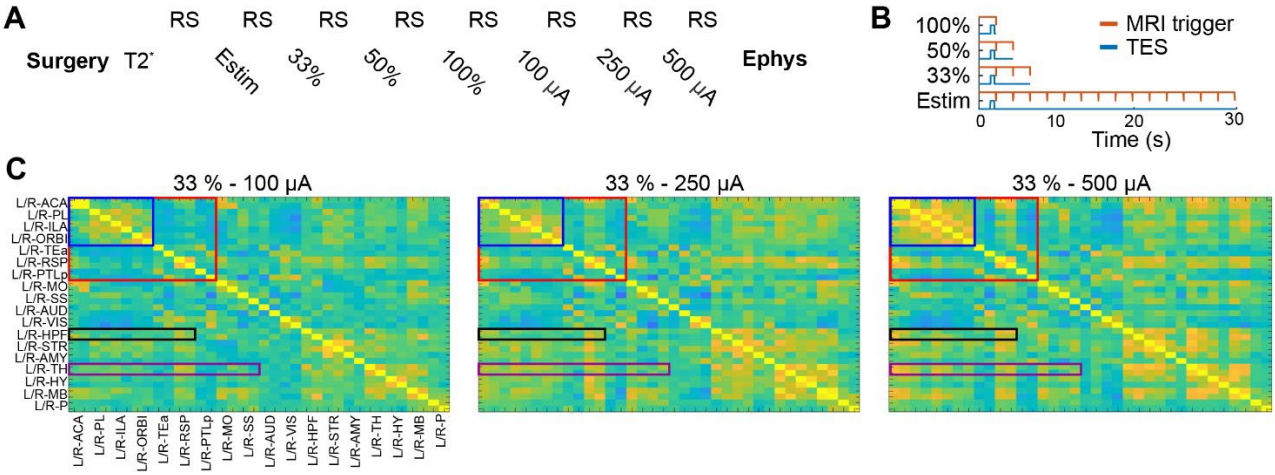

Figure 4. Combined TES-fMRI experiments in anesthetized rats. A) Anatomical and functional MRI scans are collected (RS-resting state). Imaging is followed by an electrophysiology (Ephys) experiment. **B)** Time-course of TES and image acquisition. **C)** Functional connectivity matrix shows stimulation intensity dependent changes (100 µA, 250 µA and 500 µA at 33% duty cycle, first resting state was used as baseline). Prefrontal (blue), default mode (red), cortico-hippocampal (black) and thalamo-cortical (purple) networks are shown.

Well isolated single units were recorded from the right hippocampus after BOLD-fMRI. Cells were classified into three putative cell types: narrow-interneurons, wide-interneurons, and pyramidal-cells[11]. Of the 45 isolated single units, 29 showed stimulation polarity dependent modulation of their spiking rate (Fig. 5A), verifying the effectiveness of TES in the same experiment.

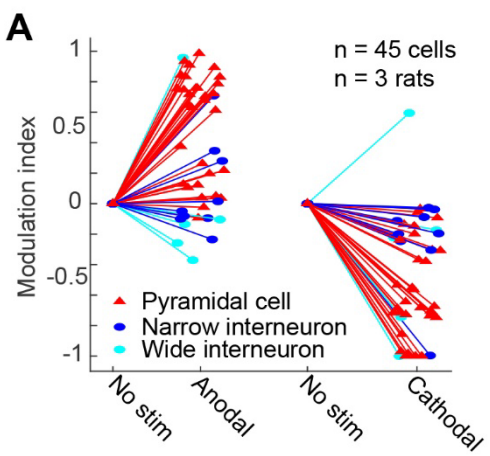

Figure 5. Electrophysiology recordings following TES-fMRI experiments. A) Firing rate changes of putative single units were opposite in a polarity dependent manner (n=45 cells in 3 rats, putative pyramidal cells, narrow and wide interneurons are shown by red triangle, blue and cyan circles, respectively). Modulation index shows the normalized change in spiking activity compared to stimulation free epochs.

Discussion: We developed an MR-compatible, deuterium-based, concurrent TES-fMRI stimulation system for rats, followed by electrophysiological verification. The effects of TES are not simply restricted to the area under the electrodes, but stimulation can also affect connectivity within cortical and cortico-subcortical networks. We found stimulation intensity-dependent changes in prefrontal, default mode, cortico-hippocampal and thalamo-cortical networks. We confirmed the functionality of our stimulation system in each rat using *in vivo*, extracellular electrophysiology. Our data can also provide insights about the relationship between neuroimaging signals and brain electrophysiology.

References:

1. *Transcranial Direct Current Stimulation in Neuropsychiatric Disorders*. (Springer International Publishing, 2021). doi:10.1007/978-3-319-33967-2.
2. Pinto, C. B., Teixeira Costa, B., Duarte, D. & Fregni, F. Transcranial Direct Current Stimulation as a Therapeutic Tool for Chronic Pain. *J. ECT* **34**, e36–e50 (2018).
3. Peterchev, A. V. *et al.* Fundamentals of transcranial electric and magnetic stimulation dose: Definition, selection, and reporting practices. *Brain Stimul.* **5**, 435–453 (2012).
4. Datta, A. *et al.* Gyri-precise head model of transcranial direct current stimulation: Improved spatial focality using a ring electrode versus conventional rectangular pad. *Brain Stimul.* **2**, 201–7, 207.e1 (2009).
5. Bikson, M. *et al.* Effect of uniform extracellular DC electric fields on excitability in rat hippocampal slices in vitro. *J. Physiol.* **557**, 175–190 (2004).
6. Esmaeilpour, Z. *et al.* Incomplete evidence that increasing current intensity of tDCS boosts outcomes. *Brain Stimul.* **11**, 310–321 (2018).
7. Esmaeilpour, Z. *et al.* Methodology for tDCS integration with fMRI. *Hum. Brain Mapp.* **41**, 1950–1967 (2020).
8. Ghobadi-Azbari, P. *et al.* fMRI and transcranial electrical stimulation (tES): A systematic review of parameter space and outcomes. *Prog. Neuro-Psychopharmacology Biol. Psychiatry* **107**, 110149 (2021).

9. Alexander, A., Lee, J. E., Lazar, M. & Field, A. S. Diffusion tensor imaging of the brain. *Neurotherapeutics* **4**, 316–329 (2007).
10. Swanson, L. W. Brain maps 4.0—Structure of the rat brain: An open access atlas with global nervous system nomenclature ontology and flatmaps. *J. Comp. Neurol.* **526**, 935–943 (2018).
11. Petersen, P., Siegle, J., Steinmetz, N., Mahallati, S. & Buzsáki, G. CellExplorer: a graphical user interface and a standardized pipeline for visualizing and characterizing single neurons. *bioRxiv* 2020.05.07.083436 (2020).